Quantitative Evaluation of L-[Methyl-C-11] Methionine Uptake in Tumor Using Positron Emission Tomography

Jun Hatazawa, Kiichi Ishiwata, Masatoshi Itoh, Motonobu Kameyama, Kazuo Kubota, Tatsuo Ido, Taiju Matsuzawa, Takashi Yoshimoto, Shoichi Watanuki, and Shinya Seo

Division of Nuclear Medicine, Division of Radiopharmaceutical Chemistry, Cyclotron and Radioisotope Center, Department of Neurosurgery, Tohoku University, School of Medicine, Department of Radiology and Nuclear Medicine, Research Institute for Tuberculosis and Cancer, Tohoku University

Tumor uptake of L-[methyl-^{11}C]methionine ([^{11}C]Met) was assessed in six patients with brain tumors and three patients with lung cancer using positron emission tomography (PET). In arterial plasma samples taken at 5, 15, 30, and 60 min after injection, a fraction of [^{11}C]Met was measured using high performance liquid chromatography in individual patients. Employing curve fitting, a history of [^{11}C]Met activity was obtained as an input function. By means of sequential PET scannings and graphic analysis, uptake rate and distribution volume of [^{11}C]Met in tumor tissue were calculated. In two studies irreversible uptake into the tumors was not seen when total plasma ^{11}C activity was used as the input; however when [^{11}C]Met plasma activity was used, definite irreversible uptake was seen, indicating tumor viability. In other studies, up to 24% underestimation of uptake rate was found. The present results demonstrated the importance of measuring [^{11}C]Met in plasma for quantitative assessment of in vivo amino acid metabolism in tumors.

J Nucl Med 30:1809–1813, 1989

Positron emission tomography (PET) using L-[methyl-^{11}C]methionine ([^{11}C]Met) as a tracer has been used to measure in vivo amino acid metabolism in human brain (*1–3*), brain tumors (*3–7*), and lung cancer (*8–10*).

Although accurate measurement of plasma radioactivity of an injected labeled amino acid, apart from its metabolites, is essential for accurate compartmental analysis, we have found no reports including such measurements in individual studies. We previously measured the metabolic products of [^{11}C]Met in human plasma during PET-methionine study and found remarkable individual differences in the clearance pattern of plasma [^{11}C]Met (*11*). Herein, we evaluate the uptake rate and distribution volume of [^{11}C]Met in brain tumors and lung cancer using graphic analysis (*12*) after correction for plasma metabolites of [^{11}C]Met in individual cases. The importance of plasma metabolite analysis for quantitative assessment is demonstrated.

MATERIALS AND METHODS

Patients

Six patients with brain tumors and three patients with lung cancer were studied with positron emission tomography (PET) and [^{11}C]Met between November 1987 and December 1988. Clinical information is summarized in Table 1. All the patients with brain tumors had partial resection of tumors or stereotaxic biopsy. One patient with lung cancer (ID 590) was studied twice during radio- and chemotherapy. Each patient fasted prior to the study. The dose of whole-body radiation was 12 mrad/mCi of [^{11}C]Met in an adult man with a body weight of 70 kg (*13*). Informed consent was obtained from the patients or the parents (ID 714). The present project was approved by the Committee for Clinical PET Study of Tohoku University.

Scanner and Procedure

ECAT II (EG&G, Ortec) (*14*) and PT-931 (CTI, Knoxville, TN) (*15*) were employed. The spacial resolution of the image

Received Feb. 13, 1989; revision accepted June 27, 1989.

For reprints contact: Jun Hatazawa, MD, PhD, Cyclotron and RI Center, Tohoku University, Aramaki Aoba, Sendai, Japan.

TABLE 1
Patient Data

ID	Age/sex	Scanner	Disease	Pathology	Therapy before PET
552	72 M	PT931	Lung cancer	Squamous cell carcinoma	Radio- and chemotherapy
590	39 M	ECAT II	Lung cancer	Adenocarcinoma	Radiotherapy (42 Gy)
590	39 M	ECAT II	Lung cancer	Adenocarcinoma	Radiotherapy (69 Gy) Chemotherapy
600	49 M	ECAT II	Brain tumor	Astrocytoma grade II	Radio- and chemotherapy
606	61 F	ECAT II	Lung cancer	Oat cell carcinoma	None
619	28 M	PT931	Brain tumor	Neuroblastoma	None
629	46 F	PT931	Brain tumor	Astrocytoma grade II	Radiotherapy
714	16 F	PT931	Brain tumor	Glioblastoma	Radiotherapy (50 Gy)
333	40 M	PT931	Brain tumor	Astrocytoma grade II	Radio- and chemotherapy
758	63 M	PT931	Brain tumor	Glioblastoma	None

was 15 mm and 8 mm for the ECAT II and PT-931, respectively, and slice thickness was 18 and 9 mm at FWHM, respectively. Three to four images were obtained with the ECAT II at 1 cm center-to-center spacing and 14 images were obtained with PT-931 at 8 mm spacing. The sequential scan was performed for one of these slices where the tumor was most visible in x-ray CT or MRI.

Before scanning, a short 21-gauge cannule was inserted to a brachial or radial artery for arterial blood sampling. Fourteen to 24 mCi of [^{11}C]Met were administered within 30 sec through the contralateral hand vein. Repeated scanning started just after administration. Eight to ten sequential images with 5-min data acquisition were obtained. During the scanning, 1-ml arterial blood samples were taken at 0.33, 0.67, 1, 1.5, 2.0, 2.5, 3.0, 4.0, 5.0, 7.5, 10, 15, 20, 30, 40, 50, 60 min after the i.v. administration and at the end of scanning. These blood samples were centrifuged for 3 min, and plasma samples were weighed and counted for radioactivities using a cross-calibrated well counter with ECAT II and PT-931. At 5, 15, 30, and 60 min, additional 3-ml arterial blood samples were obtained for analysis of protein-bound ^{11}C and [^{11}C]Met in plasma using high performance liquid chromatography (HPLC).

Analysis of Metabolites of [^{11}C]Met in Plasma

Protein-bound and protein-free metabolites of [^{11}C]Met in plasma were analyzed under the same conditions as described previously (*11*). Briefly, after counting total radioactivity, plasma samples taken at 3, 4, 5, 7.5, 10, 15, 20, 30, 40, 50, and 60 min after i.v. injection were treated with 5 ml of ice-cold 0.2*M* $HClO_4$ to precipitate plasma proteins. The samples were centrifuged for 3 min. The precipitate was resuspended in 5 ml of 0.2*M* $HClO_4$, and centrifuged again. This washing procedure was repeated twice. The final precipitate, counted for radioactivity and corrected for decay, was considered to be the protein-bound fraction.

For the samples taken at 5, 15, 30, and 60 min, supernatants obtained with the procedure described above were combined as a protein-free fraction. Radioactivity of this fraction was then measured. The supernatant was applied to an Aminex A-6 column. The column was eluted with 0.2 N sodium citrate. The column was reequilibrated and the elution profile was measured with a radioactivity monitor (Ramona-D equipped with an IM-2020X flow cell, Raytest). The collected effluent in 1.0 ml fraction was then counted for radioactivity with a well counter.

Uptake Rate and Distribution Volume of [^{11}C]Met

We obtained three different input functions of ^{11}C radioactivity for each study, total ^{11}C radioactivity, protein-free ^{11}C (total minus protein-bound fraction) and radioactivity for [^{11}C]Met. For total ^{11}C in plasma, integrated radioactivity from injection time to midway in each sequential scanning was calculated using a BLD computer program (*16*). For protein-free ^{11}C and [^{11}C]Met, plasma radioactivity against sampling time was fitted best to double exponential curves using the Damped Gaus Newton method.

A small fraction of serin was found in the HPLC analysis. This fraction was not considered as an input because the brain uptake index of serin is almost one-fourth of that of methionine (*17*).

As only a low percentage of protein-free metabolites and an undetectable amount of protein-bound metabolites were found in the samples taken at 5 min after administration, total radioactivity before 5 min was incorporated as a protein-free fraction and [^{11}C]Met fraction for curve fitting. The integrated radioactivity from injection time to the midtime of scanning and the radioactivity at the midpoint were obtained using these fitted curves.

The PET images were reconstructed using a measured attenuation correction, and radioactivity concentration in each pixel was converted to nCi/ml unit. Oval regions of interest were located on brain tumors and brain matter in the contralateral hemisphere in the sequential images. For lung tumors, regions of interest were superimposed on the tumor masses which were visible in the transmission images.

Plasma and tissue time-activity curves were treated with graphic analysis which enables evaluation of the unidirectional transfer process (*12*). The operational equation is

$$\frac{C_i(T)}{C_p(T)} = K_i \frac{\int_0^T C_p(t)dt}{C_p(T)} + V_p$$

where Ci(T) is the total amount of ^{11}C radioactivity at time T

TABLE 2
Ratio of protein free ^{11}C and [^{11}C]Met to total ^{11}C in Plasma at 15 min, 30 min, and 60 min After Administration

ID	Ratio of protein free ^{11}C			Ratio of [^{11}C]Met		
	15 min	30 min	60 min	15 min	30 min	60 min
552	0.99	0.83	0.43	0.93	0.70	0.29
590	0.75	0.31	0.26	0.67	0.21	0.09
590	0.91	0.54	0.26	0.80	0.44	0.16
600	0.95	0.83	0.67	0.93	0.72	0.48
606	1.00	0.87	0.43	0.96	0.74	0.24
619	1.00	0.81	0.54	0.85	0.65	0.34
629	1.00	0.93	0.63	0.91	0.75	0.33
714	1.00	0.99	0.66	0.92	0.85	0.42
333	1.00	0.98	0.87	0.97	0.89	0.72
758	1.00	0.94	0.65	0.96	0.78	0.49
Mean	0.96	0.80	0.54	0.89	0.67	0.36
s.d.	0.08	0.20	0.18	0.09	0.19	0.17

in the tissue, K_i is the rate constant for tracer transfer from the blood to the tissue of interest, Cp(T) is the tracer concentration in blood at time T, and V_p is the distribution volume of tracer. When a linear portion of the curve was identified, the slope (K_i) and the intercept (V_p) were calculated.

RESULTS

Table 2 shows the ratios of protein-free ^{11}C and [^{11}C] Met to total ^{11}C at 15, 30 and 60 min in each study. The mean radioactivity ratio of plasma [^{11}C]Met to total ^{11}C was 0.89 (s.d. = 0.09) at 15 min, 0.67 (s.d. = 0.19) at 30 min and 0.36 (s.d. = 0.17) at 60 min after administration. There were marked individual differences in the clearance rate of plasma [^{11}C]Met.

Tissue distribution of the tracer injected in a patient with a brain tumor (ID 619) and in another patient with lung cancer (ID 552) is shown in Figure 1. Besides the initial distribution of [^{11}C]Met in large vessels, accumulations in tumor tissue were visualized in both cases.

Figure 2 illustrates the graphic analysis of brain tumors and lung cancer for total ^{11}C and [^{11}C]Met in plasma as an input function. The slopes for total ^{11}C and [^{11}C]Met were visually identical in four patients (ID 552, 606, 333 and 758). In two studies (ID 590-1, 590-2), it was difficult to find a linear part in the plots without metabolite correction. In four cases (ID 600, 619, 629, and 714), there was a discrepancy of the slopes obtained with and without such correction. Table 3 shows uptake rates and distribution volumes for [^{11}C] Met in plasma as an input. In one case of lung cancer (ID 590), the values were calculated only after metabolite correction.

Mean uptake rate (min^{-1}) and distribution volume (ml/ml tissue) in the contralateral brain matter before metabolite correction was 0.019 (s.d. = 0.006) and 0.41 (s.d. = 0.16), respectively. After metabolite correction,

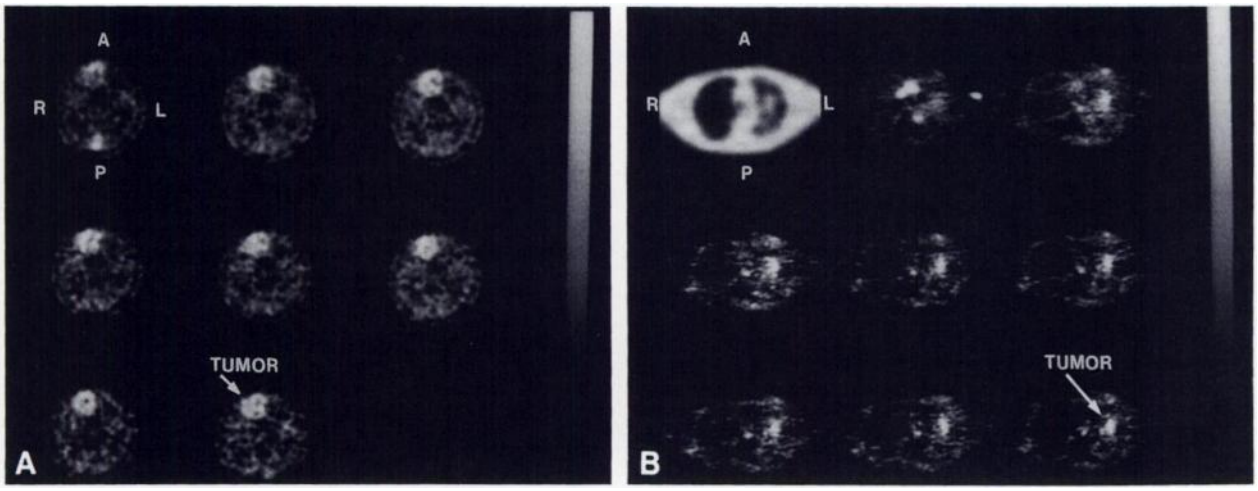

FIGURE 1
Sequential images of brain tumor (ID 619, 1A) and lung cancer (ID 552, 1B) are shown from the top left to the bottom right in order of scanning. In both studies, increased radioactivities in the tumor indicated by an arrow were observed. However, it is difficult to evaluate [^{11}C]Met incorporated in protein synthesis. In 1B, transmission image of the chest is also shown. A; anterior, P; posterior, R; right, L; left.

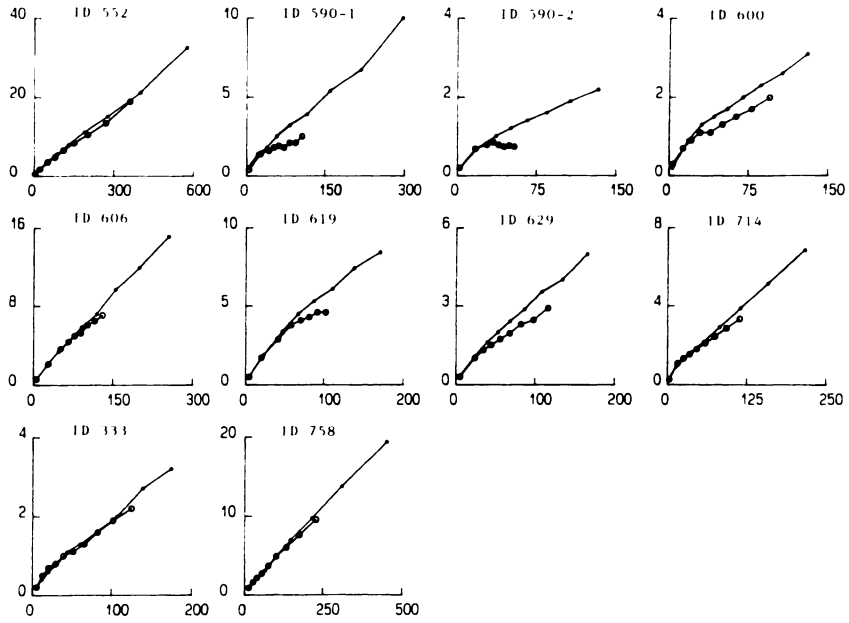

FIGURE 2
Graphic analysis of all the patients obtained for [^{11}C]MET (●) and total ^{11}C (O) as an input. abscissa: normalized time (min) ordinate: Ci(t)/Cp(t).

mean uptake rate and distribution volume changed to 0.022 (s.d. = 0.008) and 0.36 (s.d. = 0.09), respectively.

DISCUSSION

As realized by Lundqvist et al. (*18*) and Ishiwata et al. (*11*), the fraction of [^{11}C]Met in plasma decreased significantly after venous administration. Carbon-11 activity was detected in the protein fraction and in the protein-free fraction (methionine, serine, and unknown origin). Therefore, when the total amount of ^{11}C activity in plasma is employed as an input function, serious error in measurement of physiologic parameters might be anticipated.

Bergstrom et al. (*6*) estimated methionine accumulation in glioma and normal brain tissue using graphic analysis. In their study, plasma radioactivity was corrected mathematically for labeled plasma proteins by subtracting a fraction according to Lundqvist et al. (*18*). However, as reported here, there was large variation in the clearance pattern of [^{11}C]Met among individuals. Another group (*7*) evaluated the slope and intercept of the initial straight line of the plot after administrating [^{11}C]Met to avoid the presence of plasma metabolites in the late phase of the study. However, an irreversible fraction of total radioactivities in the tumor or [^{11}C]Met incorporated into protein might increase during scanning. For example, Ishiwata et al. reported that only 42% of radioactivity in rat tumor was incorporated into proteins at 5 min after [^{11}C]Met injection and then the percentage increased to 72.4% at 30 min and 76.8% at 60 min (*19*). Therefore, more reliable values for incorporated [^{11}C]Met could be obtained by measuring tissue radioactivities as long as possible.

TABLE 3
Uptake Rate and Distribution Volume of [^{11}C]Met in Tumor Calculated for Total ^{11}C and for [^{11}C]Met in Plasma

ID	Uptake rate (min^{-1})		Distribution volume (ml/ml tissue)	
	total ^{11}C	^{11}C-Met	total ^{11}C	^{11}C-Met
552	0.052	0.056	0.67	0.69
590	—	0.025	—	0.81
590	—	0.017	—	0.34
600	0.015	0.019	0.56	0.66
606	0.058	0.058	0.48	0.48
619	0.026	0.028	0.35	0.34
629	0.021	0.028	0.55	0.48
714	0.024	0.029	0.69	0.59
333	0.016	0.017	0.29	0.22
758	0.040	0.042	0.60	0.47

When protein-free ^{11}C radioactivity was employed as an input function, the magnitude of error was much smaller than that obtained for total ^{11}C. However, values still ranged from 0.3% to 12% with a mean difference of 6%. This might suggest that protein-free ^{11}C, which was much easier to measure than [^{11}C]Met with HPLC, could not be substituted for [^{11}C]Met as input when accurate measurements are requested.

We previously reported that ^{11}C activity in the tumor corrected for administered dose and body weight, a differential uptake ratio (DUR), was an indicator of tumor viability (*8*). The uptake rate obtained in this study was significantly correlated with DUR value ($p < 0.05$). However, DUR included no information regarding the fraction of incorporated [^{11}C]Met. Tumor viability should be evaluated by an irreversible fraction of [^{11}C]Met incorporated into amino acid.

In conclusion, because of considerable variations in

clearance patterns of administered [^{11}C]Met, the corrections for plasma metabolites should be performed to obtain [^{11}C]Met plasma radioactivity as an input when quantitative information regarding methionine metabolism is extracted in the PET study.

REFERENCES

1. Bustany P, Sargent T, Saudubray JM, Henry JF, Comar D. Regional human brain uptake and protein incorporation of [^{11}C]L-methionine studied in vivo with PET. *J Cereb Blood Flow Metab* 1 (suppl) 1981; I9–I10.
2. Comar D, Saudubray JM, Duthilheul A, et al. Brain uptake of 11-C-L-methionine in phenylketonuria. *Eur J Pediatr* 1981; 136:13–19.
3. Bustany P, Henry JF, de Rotrou J, et al. Correlations between clinical state and positron emission tomography measurements of local protein synthesis in Alzheimer's dementia, Parkinson's disease and gliomas. In: Greits T, Ingvar DH, Widen L, eds. The metabolism of human brain studied with positron emission tomography. New York: Raven Press, 1985: 241–249.
4. Ericson K, Lilja A, Bergstrom M, et al. Positron emission tomography with [^{11}C] methionine, [^{11}C]D-glucose, and [^{68}Ga]EDTA in the examination of supratentorial tumors. *J Comput Assist Tomogr* 1985; 9:683–689.
5. Lilja A, Bergstrom K, Hartvig P, et al. Dynamic study of supratentorial gliomas with L-methyl-11-C-methionine and positron emission tomography (PET). *AJNR* 1985; 6:505–514.
6. Bergstrom M, Ericson K, Hagenfeldt L, et al. PET study of methionine accumulation in glioma and normal brain tissue: competition with branched chain amino acids. *J Comp Assist Tomogr* 1987; 11:208–213.
7. O'Tuama LA, Guilarte TR, Douglass KH, et al. Assessment of [^{11}C]-L-methionine transport into the human brain. *J Cereb Blood Flow Metab* 1988; 8:341–345.
8. Kubota K, Matsuzawa T, Ito M, et al. Lung tumor imaging by positron emission tomography using C-11 L-methionine. *J Nucl Med* 1985; 26:37–42.
9. Fujiwara T, Matsuzawa T, Kubota K, et al. Relationship between histologic type of primary lung cancer and carbon-11-methionine uptake with positron emission tomography. *J Nucl Med* 1989; 30:33–37.
10. Kubota K, Matsuzawa T, Fujiwara T, et al. Differential diagnosis of solitary pulmonary nodules with positron emission tomography using [^{11}C]L-methionine. *J Comp Assist Tomogr* 1988; 12:794–796.
11. Ishiwata K, Hatazawa J, Kubota K, et al. Pharmacokinetics of the metabolites of L-[methyl-^{11}C] methionine in human plasma. *Eur J Nucl Med* 1989: in press.
12. Patlak CS, Blasberg RG, Fenstermacher JD. Graphical evaluation of blood to brain transfer constants from multiple-time uptake data. *J Cereb Blood Flow Metab* 1983; 3:1–7.
13. Stalnacke CG. Acta universitatis upsaliensis, 1984. No. 756.
14. Phelps ME, Hoffman EJ, Huang SC, Kuhl DE. ECAT: a new computerized tomographic imaging system of positron emitting radio-pharmaceuticals. *J Nucl Med* 1978; 19:635–647.
15. Spinks TJ, Guzzardi R, Bellina CR. Performance characteristics of a whole-body positron tomograph. *J Nucl Med* 1988; 29:1833–1841.
16. Carson RE, Huang SC, Phelps ME. BLD—a software system for physiological data handling and model analysis. *Proceedings of Fifth Annual Symposium on Computer Application in medical care. IEEE Computer Society*, 1981:562–565.
17. Oldendorf WH. Brain uptake of radiolabeled amino acids, amines, and hexoses after arterial injection. *Am J Physiol* 1971; 221:1629–1639.
18. Lundqvist H, Stalnacke CG, Langstrom B, Jones B. Labeled metabolites in plasma after intravenous administration of [^{11}CH3]-1-methionine. In: Greitz T, Ingvar DH, Widen L, eds. *The metabolism of the human brain studied with positron emission tomography.* New York: Raven Press, 1985:233–240.
19. Ishiwata K, Vaalburg W, Elsinga PH, et al. Comparison of L-[1-^{11}C]methionine and L-methyl-[^{11}C] methionine for measuring in vivo protein synthesis rate with PET. *J Nucl Med* 1988; 29:1419–1427.